

SPATIAL DISTRIBUTION SHIFTS OF *LITHOSPERMUM ERYTHORRHIZON* (BORAGINACEAE), A RARE MEDICINAL PLANT IN CHINA, UNDER FUTURE CLIMATE SCENARIOS

LI, L. R.^{1#} – TANG, Y. H.^{1#} – XIANG, D. Y.² – CHEN, G. Y.² – HUANG, B.^{1*} – CHEN, T.^{1*}

¹*School of Pharmaceutical Sciences, Hunan University of Medicine, Huaihua, Hunan 418000, China*

²*Department of Traditional Chinese Medicine, Shandong College of Traditional Chinese Medicine, Yantai, Shandong 264199, China*

[#]*These authors contributed equally to this work*

^{*}*Corresponding authors*

e-mail: huangbin@hnmu.edu.cn; chenting@hnmu.edu.cn

(Received 18th Apr 2025; accepted 16th Jun 2025)

Abstract. *Lithospermum erythrorhizon*, a second-level protected wild plant in China, faces population decline and extinction risk due to medicinal overexploitation. This study integrates 209 distribution points and 37 environmental variables using Pearson correlation, MaxEnt modeling, and ArcGIS to identify key distribution drivers and project spatial shifts under current/future climates. Results show dominant factors include annual precipitation (570.5~1497.4 mm), annual mean temperature (9.2~18.4°C), coldest quarter precipitation (21.3~190.2 mm), wettest quarter precipitation (347.4~692.0 mm), and mean diurnal range (7.1~11.0°C). The high-accuracy MaxEnt model (AUC > 0.8) indicates current suitable habitats (403.09 × 10⁴ km²) concentrate in central/eastern Guizhou, Qinling-Daba Mountains, northwestern Hubei, and parts of northern China. Future projections reveal habitat expansion with southwestward migration to higher elevations: under SSP126, the centroid shifts southwest 820.16 km then northeast 134.25 km; under SSP585, it shifts southwest 865.98 km then southeast 46.41 km. This latitudinal gradient response mechanism provides critical environmental thresholds for cultivation site selection. The proposed habitat optimization strategy balances ecological protection and economic benefits through wild resource substitution while ensuring cultivated medicinal quality stability, supporting medicinal plant diversity conservation and sustainable utilization.

Keywords: *second-level protected wild plant, MaxEnt, ArcGIS, geographical distribution, centroid migration*

Introduction

Contemporary climate change is altering global ecosystem patterns at an unprecedented rate. According to projections from the Intergovernmental Panel on Climate Change (IPCC) Sixth Assessment Report, the global average temperature is expected to increase by 1.4 to 4.4°C by the end of this century, depending on different scenarios (SSP126 to SSP585). This warming is accompanied by a significant rise in the frequency and intensity of extreme weather events, which pose a direct threat to the integrity of species habitats (Vásquez-Aguilar et al., 2024). The accelerated loss of biodiversity not only undermines ecosystem services but also exacerbates complex risks to public health and resource sustainability through various pathways (Ayejoto et al., 2023), including changes in species distribution patterns (Song et al., 2023), disruption of interspecies interaction networks (Luan et al., 2024), and an increased risk of zoonotic disease transmission (Martinez et al., 2024). In this context, the integration of

species distribution models (SDMs) with niche dynamics analysis has become a critical scientific foundation for developing climate-adaptive conservation strategies, particularly in the planning of conservation efforts for endangered species and key ecological niche species (Ashrafzadeh et al., 2022; Zhang and Wang, 2023; Thompson et al., 2023).

Lithospermum erythrorhizon, commonly known as purple gromwell, is a perennial herbaceous plant belonging to the *Boraginaceae* family (Auber et al., 2020). It is commonly found in China at elevations ranging from 50 to 2500 m, thriving in environments with ample sunlight and good drainage, and demonstrating strong drought resistance. This species is also distributed in East Asia, including countries such as South Korea and Japan, where it is widely utilized as a traditional medicinal plant (Choi et al., 2016; Yoon et al., 2017). The roots of *L. erythrorhizon* are the primary medicinal part, rich in secondary metabolites such as shikonin, which confer environmental adaptation benefits and enhance the plant's tolerance to abiotic stresses (Tatsumi et al., 2023). *L. erythrorhizon* holds significant importance within the framework of traditional Chinese medicine, serving both medicinal and natural dyeing functions (Kumar et al., 2021). Modern pharmacological studies have confirmed that this medicinal material is rich in naphthoquinone compounds, such as shikonin, which exhibit notable activities in anti-inflammatory, anti-tumor, and wound healing processes (Gao et al., 2023; Zhu et al., 2022; Jia et al., 2022). According to the Pharmacopoeia of China, the medicinal part of *L. erythrorhizon* is the dried root, and its medicinal sources include *Arnebia euchroma* and *Arnebia guttata*. Among these, *Arnebia euchroma* is the primary source of *L. erythrorhizon* due to its higher content of active compounds (Kumar et al., 2021), such as alkannin and shikonin derivatives. However, wild populations of *Arnebia euchroma* are currently endangered due to overharvesting and were listed in the "National Key Protected Wild Plants of China (Level II)" in 2021. Assessments of its genetic diversity indicate a decline in genetic resources in certain populations (Zhao et al., 2024). Therefore, there is an urgent need to enhance the conservation of wild *L. erythrorhizon* from the perspectives of cultural heritage, scientific advancement, and biodiversity protection. This study aims to predict the current and future potential geographical distribution of *L. erythrorhizon* under the dual pressures of climate change and human activities, as well as to identify the key environmental factors influencing its distribution in China. The findings will provide a theoretical basis for the artificial cultivation of high-quality *L. erythrorhizon*, thereby alleviating ecological pressure on wild populations and promoting sustainable utilization.

SDMs provide quantitative tools for analyzing the dynamic changes in biogeographical patterns and predicting future distribution trends by integrating species distribution data with ecological relationships among environmental variables (Carbeck et al., 2022; Hosseini et al., 2024). Among these models, the Maximum Entropy model (MaxEnt) has emerged as a key tool for identifying priority conservation areas for endangered plants due to its efficient analysis of small sample sizes and its robust representation of complex environmental relationships (Zhang et al., 2025). Current research is focusing on coupling data from the CMIP6 multi-climate scenarios (such as SSP126 and SSP585). This framework quantifies the climatic differences driven by various Shared Socioeconomic Pathways (such as low-carbon transitions versus fossil fuel-dependent development), allowing for precise assessments of the combined impacts of human activities and climate change on species distributions (Dyderski et al., 2025; Khan et al., 2024).

This study focuses on *L. erythrorhizon*, integrating the MaxEnt model with ArcGIS spatial analysis techniques to address the following scientific questions: (1) What are the key environmental drivers that constrain the geographical distribution patterns of *L. erythrorhizon*. (2) How do the suitable habitats for *L. erythrorhizon* shift and reconstruct spatially under the climate scenarios of SSP126 (sustainable pathway) and SSP585 (high-emission pathway) during the 2050s and 2090s. By analyzing the response mechanisms of *L. erythrorhizon* populations to climate change, the findings of this study will provide theoretical support and practical guidance for establishing a dynamic monitoring system for *L. erythrorhizon* resources, formulating conservation strategies for wild populations, and optimizing the medicinal quality of artificially cultivated *L. erythrorhizon* through environmental factors regulation.

Materials and methods

Species data acquisition and processing

Geographical distribution data for *L. erythrorhizon* were collected from three databases: the Chinese Virtual Herbarium (CVH, <http://www.cvh.ac.cn>), the National Specimen Information Infrastructure (NSII, <http://www.nsii.org.cn/2017/home.php>), and the Global Biodiversity Information Facility (GBIF, <https://www.gbif.org/>). Latitude and longitude coordinates for all samples were compiled into a CSV file and imported into ArcGIS (version 10.8). To reduce spatial autocorrelation, we utilized the “Spatially Rarefy Occurrence Data for SDMs” function within the “SDM Toolbox” to eliminate samples that were located less than 5 km apart (Yang et al., 2023). As shown in *Figure 1*, a total of 209 sample points were retained for subsequent modeling.

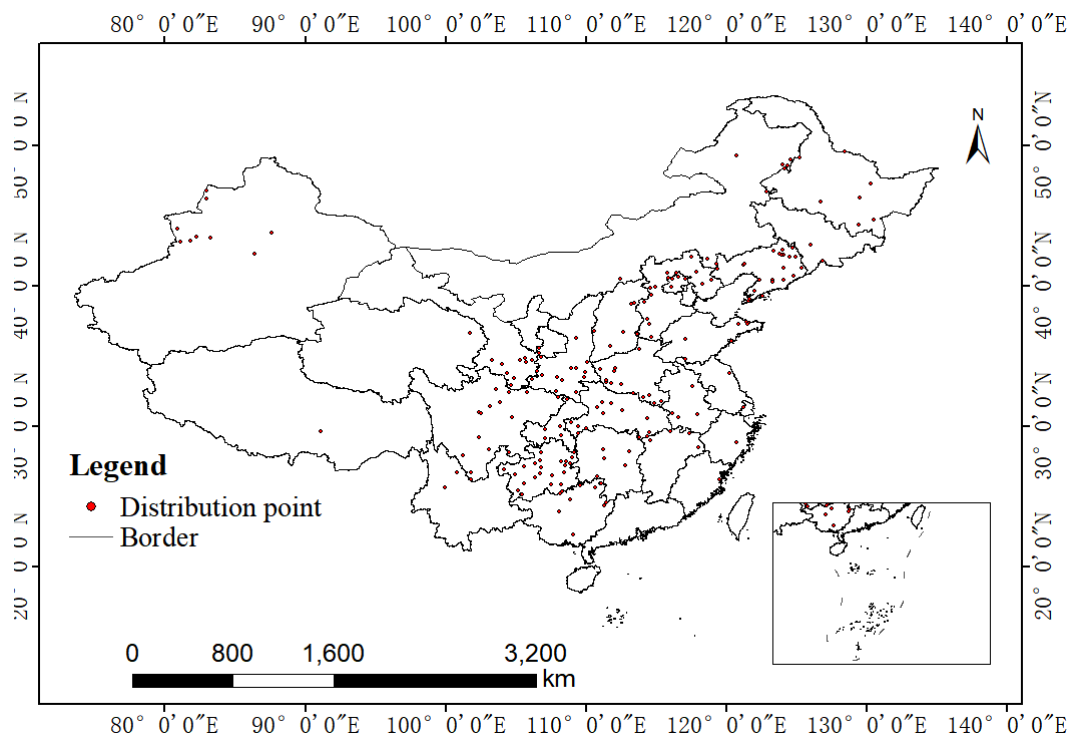


Figure 1. Distribution information of *Lithospermum erythrorhizon*

Optimization of environmental variables

Bioclimatic data were sourced from the WorldClim database (<http://www.worldclim.org/>) at a resolution of 2.5 arc minutes, encompassing 19 bioclimatic variables representative of both current (1970-2000) and projected future climate scenarios. The BCC-CSM2-MR model, noted for its strong performance in simulating climatic conditions in China, was employed to forecast future climate changes (Wu et al., 2019). Two Shared Socioeconomic Pathways (SSPs) were selected from the BCC-CSM2-MR model: a low carbon emission scenario (SSP126) and a high carbon emission scenario (SSP585). Each SSP was further divided into two distinct time frames: the 2050s (2041-2060) and the 2090s (2081-2100). Soil and topographic data were obtained from the Harmonized World Soil Database (<https://www.fao.org/soils-portal/data-hub/soil-maps-and-databases/harmonized-world-soil-database-v12/en/>) and the WorldClim database (<http://www.worldclim.org/>). The details of the thirty-seven environmental variables are presented in *Table 1*. Utilizing the geographical distribution of *L. erythrorhizon* and iterative calculations performed with MaxEnt software (version 3.4.4) based on current environmental variables, we identified environmental variables with contribution rates exceeding 0. The “Sampling” function in ArcGIS was subsequently employed to extract the values of these selected variables. Finally, a Pearson correlation analysis of the environmental variables was conducted using SPSS software (version 26). Environmental variables exhibiting absolute correlation coefficients greater than 0.8 and low contribution rates were excluded to reduce the potential adverse effects of collinearity on the model (Hao et al., 2024). The remaining environmental variables were utilized in the subsequent modeling processes.

Predictive modeling and data analysis

This study utilized 209 geographic distribution records of *L. erythrorhizon* and 20 environmental variables, which were analyzed using the MaxEnt modeling approach. The parameters were configured as follows: 75% of the occurrence data was allocated to the training dataset, while the remaining 25% was designated as the test dataset. The maximum number of background points was set to 10,000, and the maximum number of iterations was established at 1,000,000, with 10-fold cross-validation implemented. The accuracy of the MaxEnt model was evaluated by calculating the area under the receiver operating characteristic curve (AUC), which ranges from 0 to 1. The contribution and significance of environmental factors were assessed using a Jackknife test, and the optimal ranges indicated by the response curves of these factors were identified (Wang et al., 2018). The ASCII files generated from the MaxEnt prediction analysis represented the probability of occurrence of *L. erythrorhizon*, denoted as P, with values ranging from 0 to 1. A threshold of $P \geq 0.5$ was established to define the optimal suitable range of important environmental factors, with the peak probability of occurrence serving as the adaptive threshold for these factors (Zhang et al., 2022a). The ASCII files were subsequently imported into ArcGIS and converted into raster files. The Reclassify function in the raster calculator of the Spatial Analyst Tools was utilized to merge the predictions. The resulting suitability index was categorized into four classes using Jenks’ natural breaks method: non-suitable habitat (0~0.1), low-suitable habitat (0.1~0.3), moderately suitable habitat (0.3~0.5), and highly suitable habitat

(0.5~1) (Brismar, 1991). Finally, the attribute table of the reclassified files was used to calculate the ratio of grid counts for each class to the total number of grids, thereby estimating the potential habitat area for *L. erythrorhizon*.

Table 1. The details of the thirty-seven environmental variables

Variables	Name	Unit
BIO_1	Annual mean temperature	°C
BIO_2	Mean diurnal temperature range	°C
BIO_3	Isothermality	/
BIO_4	Temperature seasonality	/
BIO_5	Maximum temperature of the warmest month	°C
BIO_6	Minimum temperature of the coldest month	°C
BIO_7	Mean temperature of the wettest quarter	°C
BIO_8	Mean temperature of the wettest quarter	°C
BIO_9	Mean temperature of the driest quarter	°C
BIO_10	Mean temperature of the warmest quarter	°C
BIO_11	Mean temperature of the coldest quarter	°C
BIO_12	Annual precipitation	mm
BIO_13	Precipitation of the wettest month	mm
BIO_14	Precipitation of the driest month	mm
BIO_15	Precipitation seasonality	/
BIO_16	Precipitation of the wettest quarter	mm
BIO_17	Precipitation of the driest quarter	mm
BIO_18	Precipitation of the warmest quarter	mm
BIO_19	Precipitation of the coldest quarter	mm
Awc_class	Soil available water content	%
Slope	Slope	°
Elev	Elevation	m
Aspect	Aspect	/
T_ph_h2o	Topsoil pH	-log(H ⁺)
S_ph_h2o	Subsoil pH	-log(H ⁺)
T_oc	Topsoil organic carbon content	%weight
S_oc	Subsoil organic carbon content	%weight
T_clay	Topsoil clay content	%weight
S_clay	Subsoil clay content	%weight
T_sand	Topsoil sand content	%weight
S_sand	Subsoil sand content	%weight
T_silt	Topsoil silt content	%weight
S_silt	Subsoil silt content	%weight
T_ece	Topsoil electrical conductivity	ds/m
S_ece	Subsoil electrical conductivity	ds/m
T_caco3	Topsoil carbonate or lime content	%weight
S_caco3	Subsoil carbonate or lime content	%weight

Centroid migration

The centroid of suitable habitat for *L. erythrorhizon* across various scenarios and periods was calculated using the “Mean Center” function in the spatial statistics module of ArcGIS. This analysis clarified the location of the centroid and the changes in the suitable habitat for *L. erythrorhizon* in response to different climate change conditions, thereby enabling a more detailed investigation of centroid migration trends (Liu et al., 2018).

Results

Modeling environmental variables and evaluation of model accuracy

A Pearson correlation analysis was conducted on 33 environmental variables (Fig. 2A). From this initial set, 20 environmental factors were selected for the construction of the MaxEnt model (Table 2). The area under the curve (AUC) metric was employed to assess the predictive performance of the model. The AUC value derived from the analysis of the receiver operating characteristic (ROC) curve for the MaxEnt model was found to be 0.895. This value, which exceeds 0.8 and approaches 0.9, indicates that the model demonstrates good performance (Astuti and Cropper, 2019). A visual representation of these results is presented in Figure 2B.

Table 2. Environmental variables for the MaxEnt model

Environmental variables	Name	Unit
Aspect	Aspect	/
Awc_class	Soil available water content	%
Elev	Elevation	m
S_caco3	Subsoil carbonate or lime content	%weight
S_clay	Subsoil clay content	%weight
S_ece	Subsoil electrical conductivity	ds/m
S_oc	Subsoil organic carbon content	%weight
S_ph_h2o	Subsoil pH	-log(H ⁺)
Slope	Slope	°
T_oc	Topsoil organic carbon content	%weight
T_sand	Topsoil sand content	%weight
T_silt	Topsoil silt content	%weight
BIO_1	Annual mean temperature	°C
BIO_2	Mean diurnal temperature range	°C
BIO_3	Isothermality	/
BIO_12	Annual precipitation	mm
BIO_15	Precipitation seasonality	/
BIO_16	Precipitation of the wettest quarter	mm
BIO_18	Precipitation of the warmest quarter	mm
BIO_19	Precipitation of the coldest quarter	mm

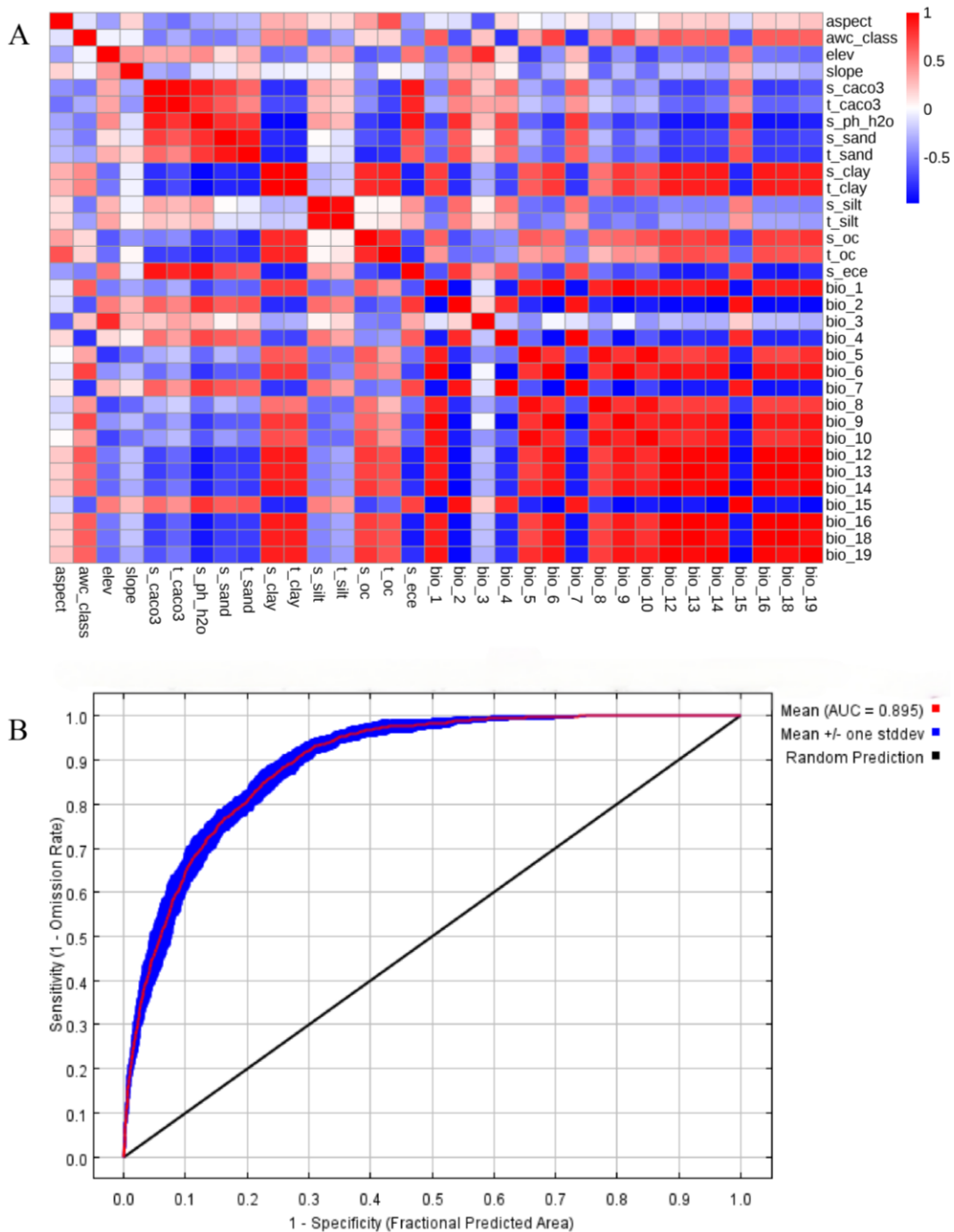


Figure 2. Modeling environmental variables and evaluation of model accuracy: correlation analysis heatmap (A); ROC curve (B)

Dominant environmental variables

The impact of environmental variables on species distribution models is primarily determined by their contributions to the model, as well as the regularized training gain associated with these variables. As illustrated in *Table 3*, under current climate scenarios, several environmental factors—including annual precipitation (BIO_12), annual mean temperature (BIO_1), precipitation of the coldest quarter (BIO_19), precipitation of the

wettest quarter (BIO_16), and mean diurnal range (BIO_2)—demonstrate relatively high contributions, with these five variables collectively accounting for 61.2% of the model’s explanatory power. Notably, BIO_12 alone contributes 30.4%. *Figure 3* depicts an analysis of regularized training gain for the environmental variables utilizing the Jackknife method. When evaluated individually, the variables that exert the most substantial influence on regularized training gain are annual precipitation (BIO_12), annual mean temperature (BIO_1), precipitation of the coldest quarter (BIO_19), precipitation of the wettest quarter (BIO_16), and mean diurnal range (BIO_2). This suggests that these five environmental variables significantly influence the potentially suitable habitat for *L. erythrorhizon*. Based on the comprehensive contribution rates and the Jackknife analysis, we have identified BIO_12, BIO_1, BIO_19, BIO_16, and BIO_2 as the five dominant environmental variables.

Suitable habitat range

The response curves of environmental variables facilitate the assessment of the relationship between the probability of occurrence and environmental variables. In this study, we utilized the MaxEnt model to investigate the optimal range of environmental variables influencing the distribution of *L. erythrorhizon* and to determine its adaptive thresholds. Given the significance of these environmental variables, we present the response curves and suitable ranges for the five most influential factors. Based on *Figure 4* and *Table 4*, it can be inferred that, using a probability of occurrence greater than 0.5 as a reference standard, the optimal ranges for *L. erythrorhizon* with respect to BIO_12, BIO_1, BIO_19, BIO_16, and BIO_2 are 570.5~1497.4 mm, 9.2~18.4°C, 21.3~190.2 mm, 347.4~692.0 mm, and 7.1~11.0°C, respectively. These findings indicate that the primary environmental variables affecting the distribution of *L. erythrorhizon* are predominantly precipitation and temperature.

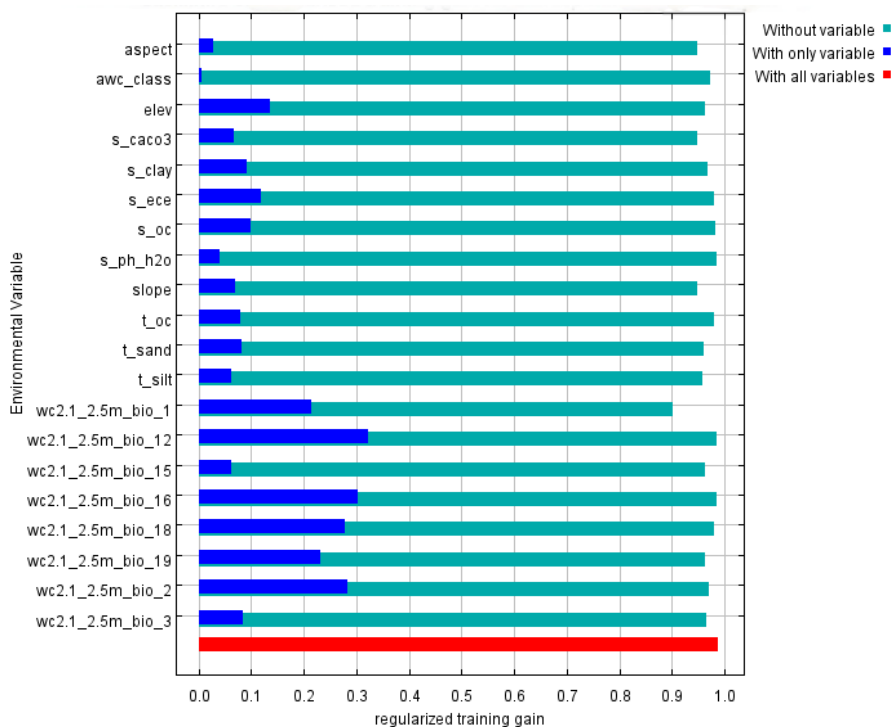


Figure 3. Gain of each variable (jackknife test)

Table 3. Environmental variables contributions

Environmental variables	Name	Percent contribution (%)
Aspect	Aspect	3.1
Awc_class	Soil available water content	0.7
Elev	Elevation	3.1
S_caco3	Subsoil carbonate or lime content	5.6
S_clay	Subsoil clay content	2
S_ece	Subsoil electrical conductivity	0.9
S_oc	Subsoil organic carbon content	1.2
S_ph_h2o	Subsoil pH	0.6
Slope	Slope	8.3
T_oc	Topsoil organic carbon content	1.2
T_sand	Topsoil sand content	2.4
T_silt	Topsoil silt content	2.3
BIO_1	Annual mean temperature	22.4
BIO_2	Mean diurnal temperature range	1.7
BIO_3	Isothermality	4.7
BIO_12	Annual precipitation	30.4
BIO_15	Precipitation seasonality	1.9
BIO_19	Precipitation of the coldest quarter	4.4
BIO_16	Precipitation of the wettest quarter	2.3
BIO_18	Precipitation of the warmest quarter	0.7

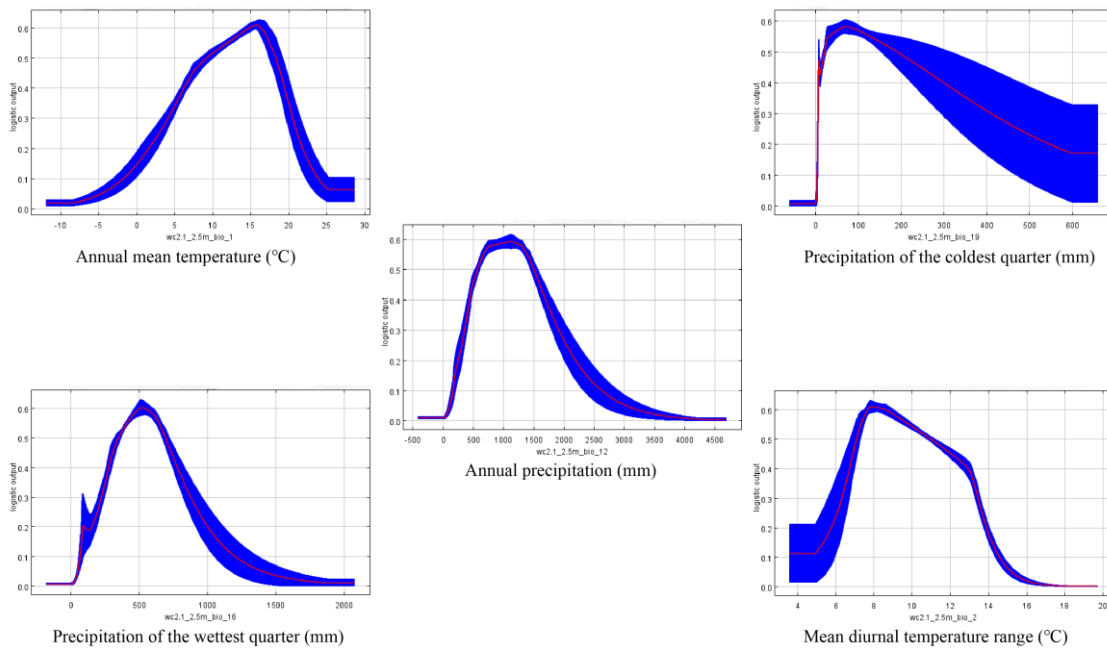


Figure 4. The response curve of dominant environmental variables

Table 4. The suitable range for the dominant environmental variables

Environmental variables	Suitable range	Adaptive threshold
BIO_12	570.5~1497.4 mm	1115.4 mm
BIO_1	9.2~18.4°C	15.8°C
BIO_19	21.3~190.2 mm	69.5 mm
BIO_16	347.4~692.0 mm	509.5 mm
BIO_2	7.1~11.0°C	7.8°C

Potential distribution under present climate

The visualization of ecological suitability classification (Fig. 5) indicates that the total area suitable for *L. erythrorhizon* is 403.09×10^4 km², comprising generally suitable areas (147.23×10^4 km²), moderately suitable areas (123.95×10^4 km²), and highly suitable areas (95.95×10^4 km²). Spatial pattern analysis reveals that the highly suitable areas for *L. erythrorhizon* exhibit a significant spatial clustering under the current climatic conditions, primarily located in the eastern region of the Yunnan-Guizhou Plateau, the boundary area between Gansu and Shaanxi, throughout Shaanxi Province, the northwest of Hubei, the southern part of Shanxi, the western region of Henan, the eastern edge of the Sichuan Basin, and in the eastern parts of Hebei and Liaoning. Additionally, scattered distributions are observed in provinces such as Hunan, Shandong, Anhui, and Zhejiang.

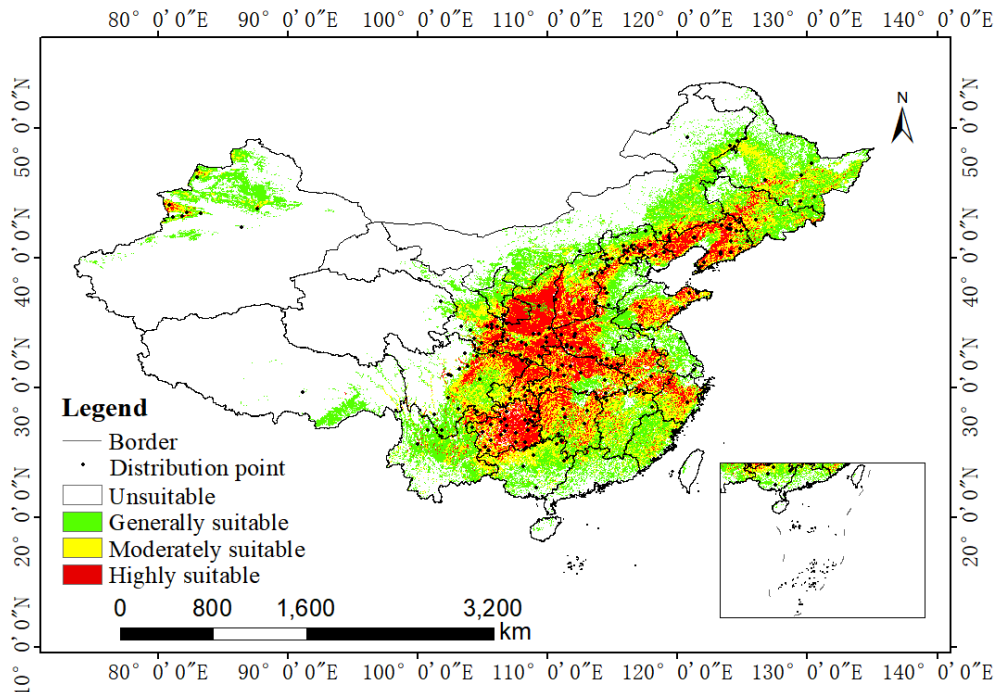


Figure 5. Potential distribution of *Lithospermum erythrorhizon* under present climate

Potential distribution under future climate

In the SSP126 scenario for the 2050s, the area of highly suitable habitat is projected to be 145.04×10 km², while the area of moderately suitable habitat is estimated at

125.08 × 10⁴ km². The total area of suitable habitat will reach 448.12 × 10⁴ km², representing an increase of 11.16% compared to the current conditions. Changes in spatial patterns indicate that regions such as Jiangsu, Anhui, Henan, Shandong, Hubei, Jilin, and southeastern Inner Mongolia will see low suitability areas transition to moderate suitability. The area of highly suitable habitat will expand into eastern Jiangsu, and the highly suitable habitat in Hunan Province will increase, with low suitability areas expanding outward. By the 2090s, the area of highly suitable habitat will slightly decrease to 138.09 × 10⁴ km², while the area of moderately suitable habitat will increase to 145.14 × 10⁴ km², resulting in a total suitable habitat area of 449.59 × 10⁴ km², which is an increase of 11.53% compared to current conditions. Compared to the 2050s, further transitions from low to moderate suitability will occur in Jiangsu, Anhui, Henan, Shandong, Hubei, Jilin, southeastern Inner Mongolia, eastern Sichuan, and western Zhejiang, with low suitability areas continuing to expand outward, and highly suitable habitats covering eastern Jiangsu and eastern Zhejiang. Notably, the highly suitable habitat in the central and southern regions of Hunan Province will degrade to moderate suitability. In the SSP585 scenario for the 2050s, the area of highly suitable habitat is projected to be 136.82 × 10⁴ km², while the area of moderately suitable habitat will be 146.55 × 10⁴ km². The total area of suitable habitat will be 458.01 × 10⁴ km², reflecting an increase of 13.62% compared to current conditions. Relative to the present, regions such as Jiangsu, Anhui, Henan, Shandong, Hubei, Jilin, southeastern Inner Mongolia, eastern Sichuan, and eastern Zhejiang will see low suitability areas transitioning to moderate suitability, with the overall area of low suitability expanding outward. By the 2090s, the area of highly suitable habitat will slightly decrease to 133.83 × 10⁴ km², and the area of moderately suitable habitat will decline to 136.65 × 10⁴ km², resulting in a total suitable habitat area of 443.40 × 10⁴ km², which is an increase of 9.99% compared to current conditions. Low suitability areas in Jiangsu, Anhui, Henan, Shandong, Hubei, Jilin, southeastern Inner Mongolia, and eastern Sichuan will continue to transition to moderate suitability, with the overall area of low suitability expanding outward (Fig. 6).

Centroid migration of *L. erythrorhizon*

Under the SSP126 scenario, the centroid of the suitable habitat for *L. erythrorhizon* shifts southwest by 820.16 km by the 2050s, and then changes direction to shift northeast by 134.25 km by the 2090s. In the SSP585 scenario, the centroid also shifts southwest by 865.98 km in the 2050s, followed by a southeast shift of 46.41 km by the 2090s. Overall, the geographic distribution of *L. erythrorhizon* shows a trend of migration towards higher elevation areas in the western regions, with no significant changes in latitude (Fig. 7; Table 5).

Table 5. Changes in the centroid of *Lithospermum erythrorhizon* under different climatic scenarios over periods

Climate scenarios	Periods	Longitude (°E)	Latitude (°N)	Migration distance (km)
	Present	113.08	34.44	
SSP126	2050s	105.93	32.98	820.16
SSP126	2090s	107.02	33.40	134.25 (2050s to 2090s)
SSP585	2050s	105.70	32.40	865.98
SSP585	2090s	105.98	32.14	46.41 (2050s to 2090s)

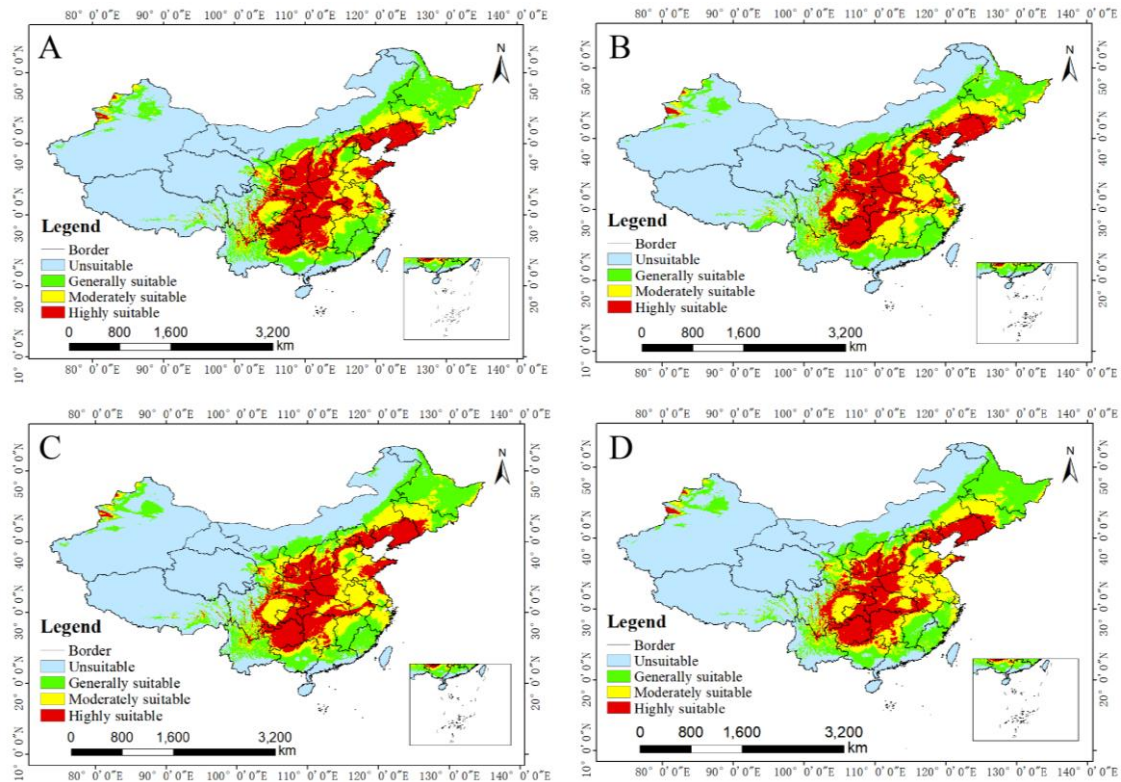


Figure 6. Potential distribution of *Lithospermum erythrorhizon* under future climate: 2041-2060, SSP 126 (A); 2081-2100, SSP 126 (B); 2041-2060, SSP 585 (C); 2081-2100, SSP 585 (D)

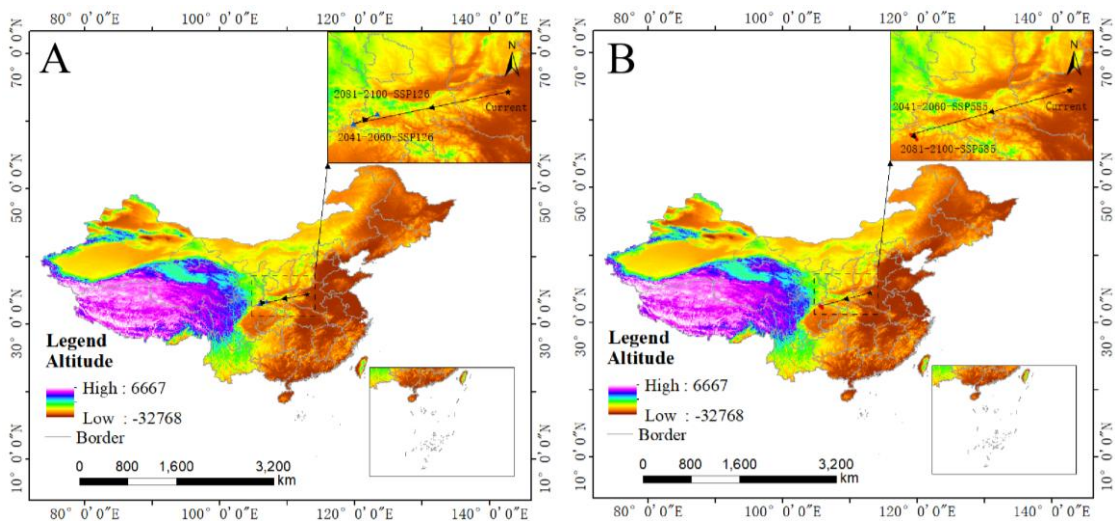


Figure 7. Centroid migration trajectories of the total suitable habitat for *Lithospermum erythrorhizon* under future climate change: 2050s -2090s, SSP126 (A); 2050s -2090s, SSP585 (B)

Discussion

The results of this study indicate that precipitation factors such as Annual Precipitation, Precipitation of the Coldest Quarter, and Precipitation of the Wettest

Quarter, along with temperature variables including Annual Mean Temperature and Mean Diurnal Range, are key climatic elements regulating the geographic distribution of *Lithospermum erythrorhizon*. Among these, temperature factors exert a decisive influence on the native distribution of *Arnebia euchroma*, as evidenced by ecological niche models that demonstrate a higher predictive weight for temperature parameters compared to other environmental variables. This finding aligns with ecological principles that suggest high-altitude species distributions are primarily driven by temperature gradients (Mohapatra et al., 2019). Specifically, temperature regulates the seed germination process during the spring and summer, as well as the efficiency of seedling establishment, thereby forming significant physiological constraints on the distribution of suitable habitats for the species (Vandelook et al., 2008). Resource surveys reveal a significant correlation between the population density of *Arnebia guttata* in Xinjiang and precipitation gradients: in arid regions with low annual precipitation, populations are sparse, whereas Bayanbaolig Town, located in an area with moderate precipitation during the warmest season, exhibits the highest population density, confirming the positive influence of moderate precipitation conditions on species growth (Liu et al., 2024). It is noteworthy that climate model predictions indicate that future warming will exacerbate soil moisture evaporation, leading to a northward shift and latitudinal contraction of suitable habitats. This trend of habitat fragmentation may disrupt the evolutionary balance of species adapted to cold climates, consequently affecting their population dispersal and niche maintenance capabilities (Wang et al., 2024; Yan et al., 2024). These findings validate the use of bioclimatic variables as quantitative indicators of ecological niche boundaries, providing a reliable framework of environmental threshold parameters for assessing species distribution dynamics under climate change.

Predictive results indicate that future climate change will significantly alter the habitat suitability patterns for *L. erythrorhizon*. Specifically, areas that were previously unsuitable are projected to gradually transform into highly suitable areas, while low-elevation areas at the margins of the species' distribution are expected to experience a decline in suitability (Bai et al., 2018). This phenomenon may be closely related to climate warming, which could push temperature and moisture conditions in low-elevation habitats beyond the ecological thresholds of the species. Many low-latitude regions may lose ecological adaptability due to excessive warming or drought conditions (Wang et al., 2024). Notably, the model suggests that the species still has the potential for range expansion in the western high-elevation areas and certain low-elevation zones. Regional climate stability and topographical heterogeneity may be critical factors in maintaining these potentially suitable areas (Yan and Tang, 2019). Theoretically, populations at lower elevations could compensate for habitat loss caused by climate stress by migrating to higher latitudes and higher elevation regions. The trajectory of centroid migration further supports the potential trend of this species expanding into higher elevations (Zhang et al., 2024). However, migration corridors in lowland areas may be obstructed due to the absence of elevation gradients, compounded by habitat fragmentation resulting from agricultural expansion, which could severely restrict actual migration capabilities.

L. erythrorhizon is an important medicinal resource plant in China. Due to overharvesting, the wild populations of this species have significantly declined and are now at risk of extinction (Zhao et al., 2024). Molecular genetic studies indicate a marked decrease in genetic diversity among the existing populations, with the majority

of genetic variation arising from differences within populations. Furthermore, gene flow indices suggest that the maintenance of genetic diversity primarily relies on intra-population gene exchange (Zhao et al., 2024). It is important to note that the synthesis of secondary metabolites in medicinal plants is highly dependent on specific habitat conditions. When cultivated outside their native habitats, the content of their characteristic active components may decrease, leading to reduced pharmacological activity (Zhang et al., 2022b). In light of this, the habitat optimization strategy proposed in this study offers dual benefits: it ensures the stability of cultivated medicinal material quality by establishing a core germplasm resource nursery (Wu et al., 2024), while also creating a “composite system of ecological planting and wild nurturing” that keeps the intensity of wild resource collection within the annual regeneration rate threshold (Zeng et al., 2024). This “wild-simulating” sustainable utilization model not only preserves the genetic integrity of medicinal plants but also enhances the synergistic value of ecosystem services and economic benefits of medicinal materials. This approach holds significant implications for the maintenance of species diversity and sustainable utilization.

Conclusions

This study utilized the MaxEnt model to analyze 37 environment variables and identified five key environmental factors influencing the distribution of *Lithospermum erythrorhizon*, along with their optimal ranges: annual precipitation (570.5~1497.4 mm), annual mean temperature (9.2~18.4°C), precipitation of the coldest quarter (21.3~190.2 mm), precipitation of the wettest quarter (347.4~692.0 mm), and mean diurnal range (7.1~11.0°C). Under current climatic conditions, the highly suitable areas for *L. erythrorhizon* in China are primarily located in the central and upper regions of Guizhou, western Shaanxi, western Henan, southern Shanxi, eastern Sichuan, eastern Shanxi, and the eastern and western parts of Liaoning, as well as eastern Hebei. Projections under future climate change scenarios indicate that the total area of suitable habitat for *L. erythrorhizon* will expand, with the distribution center shifting towards higher elevation areas in the southwest.

Acknowledgements. This work was financially supported by the Reform Project of Hunan Provincial Education Department (No. 202401001789), the Natural Science Foundation of Hunan Province (No. 2024JJ7319; No. 2025JJ70465), the doctoral research project initiation fund at Hunan University of Medicine (No. 202412).

REFERENCES

- [1] Ashrafzadeh, M. R., Khosravi, R., Mohammadi, A., Naghipour, A. A., Khoshnamvand, H., Haidarian, M., Penteriani, V. (2022): Modeling climate change impacts on the distribution of an endangered brown bear population in its critical habitat in Iran. – *Sci. Total Environ.* 837: 155753.
- [2] Astuti, I. P., Cropper, W. P. (2019): Comparing six different species distribution models with several subsets of environmental variables: predicting the potential current distribution of *Guettarda speciosa* in Indonesia. – *Biodiversitas Journal of Biological Diversity* 20.

- [3] Auber, R. P., Suttiyut, T., McCoy, R. M., Ghaste, M., Crook, J. W., Pendleton, A. L., Widhalm, J. R., Wisecaver, J. H. (2020): Hybrid de novo genome assembly of red gromwell (*Lithospermum erythrorhizon*) reveals evolutionary insight into shikonin biosynthesis. – *Hortic Res* 7: 82.
- [4] Ayejoto, D. A., Agbasi, J. C., Nwazelibe, V. E., Egbueri, J. C., Alao, J. O. (2023): Understanding the connections between climate change, air pollution, and human health in Africa: insights from a literature review. – *J Environ Sci Health C Toxicol Carcinog* 41: 77-120.
- [5] Bai, Y., Wei, X., Li, X. (2018): Distributional dynamics of a vulnerable species in response to past and future climate change: a window for conservation prospects. – *PeerJ* 6: e4287.
- [6] Brismar, J. (1991): Understanding receiver-operating-characteristic curves: a graphic approach. *AJR*. – *American Journal of Roentgenology* 157: 1119-1121.
- [7] Carbeck, K., Wang, T., Reid, J. M., Arcese, P. (2022): Adaptation to climate change through seasonal migration revealed by climatic versus demographic niche models. – *Glob Chang Biol* 28: 4260-4275.
- [8] Choi, Y. H., Kim, G. S., Choi, J. H., Jin, S. W., Kim, H. G., Han, Y., Lee, D. Y., Choi, S. I., Kim, S. Y., Ahn, Y. S., Lee, K. Y., Jeong, H. G. (2016): Ethanol extract of *Lithospermum erythrorhizon* Sieb. et Zucc. promotes osteoblastogenesis through the regulation of Runx2 and Osterix. – *Int J Mol Med* 38: 610-618.
- [9] Dyderski, M. K., Paż-Dyderska, S., Jagodziński, A. M., Puchałka, R. (2025): Shifts in native tree species distributions in Europe under climate change. – *J Environ Manage* 373: 123504.
- [10] Gao, T., Zhao, Y., Zhao, Y., He, Y., Huang, Q., Yang, J., Zhang, L., Chen, J. (2023): Curative effect and mechanisms of *Radix arnebiae* oil on burn wound healing in rats. – *Planta Med* 89: 709-717.
- [11] Hao, S., Zhang, D., Wen, Y. (2024): Potential geographical distribution of *Lagerstroemia excelsa* under climate change. – *Agriculture* 14: 191.
- [12] Hosseini, N., Ghorbanpour, M., Mostafavi, H. (2024): The influence of climate change on the future distribution of two *Thymus* species in Iran: MaxEnt model-based prediction. – *BMC Plant Biol* 24: 269.
- [13] Jia, Q., Fu, J., Gao, C., Wang, H., Wang, S., Liang, P., Han, S., Lv, Y., He, L. (2022): MrgX2-SNAP-tag/cell membrane chromatography model coupled with liquid chromatography-mass spectrometry for anti-pseudo-allergic compound screening in *Arnebiae Radix*. – *Anal Bioanal Chem* 414: 5741-5753.
- [14] Khan, T. U., Ullah, I., Hu, Y., Liang, J., Ahmad, S., Omifolaji, J. K., Hu, H. (2024): Assessment of suitable habitat of the demoiselle crane (*Anthropoides virgo*) in the wake of climate change: a study of its wintering refugees in Pakistan. – *Animals (Basel)*: 14.
- [15] Kumar, A., Shashni, S., Kumar, P., Pant, D., Singh, A., Verma, R. K. (2021): Phytochemical constituents, distributions and traditional usages of *Arnebia euchroma*: a review. – *J Ethnopharmacol* 271: 113896.
- [16] Liu, Q., Liu, H., Zhang, M., Lv, G., Zhao, Z., Chen, X., Wei, X., Zhang, C., Li, M. (2024): Multifaceted insights into the environmental adaptability of *Arnebia guttata* under drought stress. – *Front Plant Sci* 15: 1395046.
- [17] Liu, R., Wang, C., He, J., Zhang, Z. (2018): Analysis of geographical distribution of *Abies* in China under climate change. – *Bulletin of Botanical Research* 38: 37-46.
- [18] Luan, J., Li, S., Liu, S., Wang, Y., Ding, L., Lu, H., Chen, L., Zhang, J., Zhou, W., Han, S., Zhang, Y., Hättenschwiler, S. (2024): Biodiversity mitigates drought effects in the decomposer system across biomes. – *Proc Natl Acad Sci USA* 121: e2313334121.
- [19] Martinez, P. A., Teixeira, I., Siqueira-Silva, T., Da Silva, F. F. B., Lima, L. A. G., Chaves-Silveira, J., Olalla-Tárraga, M., Gutiérrez, J. M., Amado, T. F. (2024): Climate change-related distributional range shifts of venomous snakes: a predictive modelling study of effects on public health and biodiversity. – *Lancet Planet Health* 8: e163-e171.

- [20] Mohapatra, J., Singh, C. P., Hamid, M., Verma, A., Semwal, S. C., Gajmer, B., Khuroo, A. A., Kumar, A., Nautiyal, M. C., Sharma, N. (2019): Modelling *Betula utilis* distribution in response to climate-warming scenarios in Hindu-Kush Himalaya using random forest. – *Biodiversity and Conservation* 28: 2295-2317.
- [21] Song, X., Jiang, Y., Zhao, L., Jin, L., Yan, C., Liao, W. (2023): Predicting the potential distribution of the szechwan rat snake (*Euprepiophis perlacea*) and its response to climate change in the Yingjing Area of the Giant Panda National Park. – *Animals (Basel)*: 13.
- [22] Tatsumi, K., Ichino, T., Isaka, N., Sugiyama, A., Moriyoshi, E., Okazaki, Y., Higashi, Y., Kajikawa, M., Tsuji, Y., Fukuzawa, H., Toyooka, K., Sato, M., Ichi, I., Shimomura, K., Ohta, H., Saito, K., Yazaki, K. (2023): Excretion of triacylglycerol as a matrix lipid facilitating apoplast accumulation of a lipophilic metabolite shikonin. – *J Exp Bot* 74: 104-117.
- [23] Thompson, J. B., Davis, K. E., Dodd, H. O., Wills, M. A., Priest, N. K. (2023): Speciation across the Earth driven by global cooling in terrestrial orchids. – *Proc Natl Acad Sci USA* 120: e2102408120.
- [24] Vandeloos, F., Van De Moer, D., Van Assche, J. (2008): Environmental signals for seed germination reflect habitat adaptations in four temperate Caryophyllaceae. – *Functional Ecology* 22: 470-478.
- [25] Vásquez-Aguilar, A. A., Hernández-Rodríguez, D., Martínez-Mota, R. (2024): Predicting future climate change impacts on the potential distribution of the black howler monkey (*Alouatta pigra*): an endangered arboreal primate. – *Environ Monit Assess* 196: 392.
- [26] Wang, E., Lu, Z., Rohani, E. R., Ou, J., Tong, X., Han, R. (2024): Current and future distribution of *Forsythia suspensa* in China under climate change adopting the MaxEnt model. – *Front Plant Sci* 15: 1394799.
- [27] Wang, R., Li, Q., He, S., Liu, Y., Wang, M., Jiang, G. (2018): Modeling and mapping the current and future distribution of *Pseudomonas syringae* pv. *actinidiae* under climate change in China. – *PloS one* 13: e0192153.
- [28] Wu, F., Cai, G., Xi, P., Guo, Y., Xu, M., Li, A. (2024): Genetic diversity analysis and fingerprint construction for 87 passionfruit (*Passiflora* spp.) germplasm accessions on the basis of SSR fluorescence markers. – *Int J Mol Sci* 25.
- [29] Wu, T., Lu, Y., Fang, Y., Xin, X., Li, L., Li, W., Jie, W., Zhang, J., Liu, Y., Zhang, L. (2019): The Beijing Climate Center climate system model (BCC-CSM): the main progress from CMIP5 to CMIP6. – *Geoscientific Model Development* 12: 1573-1600.
- [30] Yan, C., Hao, H., Sha, S., Wang, Z., Huang, L., Kang, Z., Wang, L., Feng, H. (2024): Comparative assessment of habitat suitability and niche overlap of three *Cytospora* species in China. – *J Fungi (Basel)*: 10.
- [31] Yan, Y., Tang, Z. (2019): Protecting endemic seed plants on the Tibetan Plateau under future climate change: migration matters. – *Journal of Plant Ecology* 12: 962-971.
- [32] Yang, Y., He, J., Liu, Y., Zeng, J., Zeng, L., He, R., Guiang, M. M., Li, Y., Wu, H. (2023): Assessment of Chinese suitable habitats of *Zanthoxylum nitidum* in different climatic conditions by Maxent model, HPLC, and chemometric methods. – *Industrial Crops and Products* 196: 116515.
- [33] Yoon, J. J., Sohn, E. J., Kim, J. H., Seo, J. W., Kim, S. H. (2017): Anti-rheumatoid arthritis effect of *Kaejadan* via analgesic and antiinflammatory activity in vivo and in vitro. – *Phytother Res* 31: 418-424.
- [34] Zeng, L., Sun, Z., Fu, L., Gu, Y., Li, R., He, M., Wei, J. (2024): Cryopreservation of medicinal plant seeds: strategies for genetic diversity conservation and sustainability. – *Plants (Basel)*: 13.
- [35] Zhang, F. G., Zhang, S., Wu, K., Zhao, R., Zhao, G., Wang, Y. (2024): Potential habitat areas and priority protected areas of *Tilia amurensis* Rupr in China under the context of climate change. – *Front Plant Sci* 15: 1365264.
- [36] Zhang, H., Sun, X., Zhang, G., Zhang, X., Miao, Y., Zhang, M., Feng, Z., Zeng, R., Pei, J., Huang, L. (2022a): Potential global distribution of the habitat of endangered *Gentiana*

- rhodantha Franch: predictions based on MaxEnt ecological niche modeling. – Sustainability 15: 631.
- [37] Zhang, H., Zhou, Y., Zhang, S., Wang, Z., Liu, Z. (2025): Adaptive distribution and priority protection of endangered species *Cycas balansae*. – Plants (Basel): 14.
- [38] Zhang, H. T., Wang, W. T. (2023): Prediction of the potential distribution of the endangered species *Meconopsis punicea* Maxim under future climate change based on four species distribution models. – Plants (Basel): 12.
- [39] Zhang, X., Sun, X., Miao, Y., Zhang, M., Tian, L., Yang, J., Liu, C., Huang, L. (2022b): Ecotype division and chemical diversity of *Cynomorium songaricum* from different geographical regions. – Molecules 27.
- [40] Zhao, J., Wang, Y., Ding, W., Xu, H. (2024): Microsatellite marker-based analysis of the genetic diversity and population structure of three *Arnebiae Radix* in western China. – J Genet Eng Biotechnol 22: 100379.
- [41] Zhu, L., Li, K., Liu, M., Liu, K., Ma, S., Cai, W. (2022): Anti-cancer research on *Arnebiae radix*-derived naphthoquinone in recent five years. – Recent Pat Anticancer Drug Discov 17: 218-230.